Eur. Phys. J. Plus (2014) **129**: 34
DOI 10.1140/epjp/i2014-14034-2

THE EUROPEAN PHYSICAL JOURNAL PLUS

Regular Article

The anticipated longitudinal forces by the Biot-Savart-Grassmann-Lorentz force law are in complete agreement with the longitudinal Ampère forces

Paul G. Moyssides[a]

Physics Department, Faculty of Applied Sciences, National Technical University of Athens, Zografou Campus, 15773, Athens, Greece

Received: 4 November 2013 / Revised: 21 December 2013
Published online: 21 February 2014 – © Società Italiana di Fisica / Springer-Verlag 2014

Abstract. We explain, after 190 years to the knowledge of the author, the mechanism that creates longitudinal forces, using the Biot-Savart-Grassmann-Lorentz force law, which are found to be in complete agreement with the longitudinal forces predicted by the Ampère force law. We have also shown that a straight wire squared off at one end and pointed at the other can move in a mercury trough in the direction of the current flow by using both the Biot-Savart-Grassmann-Lorentz (B-S-G-L) and Ampère force laws. The direction of its motion is opposite to that of the pointed end. In addition we have found that the theoretically calculated velocity of the "submarine", by using both the B-S-G-L and Ampère force laws, is in complete agreement, within the error, with the one experimentally measured by the experimenters. Therefore, it has been shown that the B-S-G-L force law can anticipate longitudinal forces, which is the only aspect that distinguished these two force laws, and, thus, now, both laws are in all aspects equivalent.

1 Introduction

It was known for a long time in the scientific community that Ampère's force law, eq. (1), predicted longitudinal forces between two current elements, while the Biot-Savart-Grassmann-Lorentz (B-S-G-L) force law, eq. (2), predicted zero longitudinal forces between the same current elements. That is, these two laws were equivalent in all other aspects except for the fact that the Ampère force law predicted longitudinal forces while the B-S-G-L force law did not. This work shows the mechanism for the creation of longitudinal forces by the B-S-G-L force law and their complete agreement, within the error, with those predicted by the Ampère force law. Thus, it proves the complete equivalence between these two force laws.

In [1] the author has measured the velocity of a copper "submarine", consisting of a short piece of straight wire squared off at one end and pointed at the other, to be $v_x = 15\,\mathrm{cm/sec}$, when this is placed on the surface of a straight mercury trough conductor and a current of $I = 400\,\mathrm{A}$ flows along the mercury trough.

On the right- and on the left-hand side ends of the mercury trough, there exists a copper bar extension of trough that is 30 cm long with a cross-section of 0.5 inch × 0.5 inch. It is necessary to take into account the copper bar extensions of the trough, because they are parts of the electrical circuit and they contribute to the evaluation of the total Ampère force.

The dimensions of the copper "submarine" are: 5 cm in length and 3 mm in diameter, with a 1 cm long taper (right circular cone). The dimensions of the mercury trough are: 30 cm long with a cross-section of 0.5 inch × 0.5 inch. In our analysis we consider a 2% error in I, that is, we take: $I = (400 \pm 8)\,\mathrm{A}$. The velocity of the copper "submarine", v_x, is along the direction of the $-x$-axis, that is, in the direction of the current I.

In [1] the author states that: "the observed effects, that is the longitudinal propulsion, seem to conform with Ampère's force law, but no qualitative nor quantitative explanation has so far been found in terms of relativistic field theory or Lorentzian forces and associated Magnetohydrodynamics phenomena".

In this work: 1) We have explained the effect of the motion of the submarine in the direction of the electric current I by calculating the forces F_x along the $-x$-axis using both the Ampère and B-S-G-L force laws. It will be shown that these two forces are in complete agreement within the error. 2) We have also showed that the theoretically calculated

[a] e-mail: pmoyss@central.ntua.gr

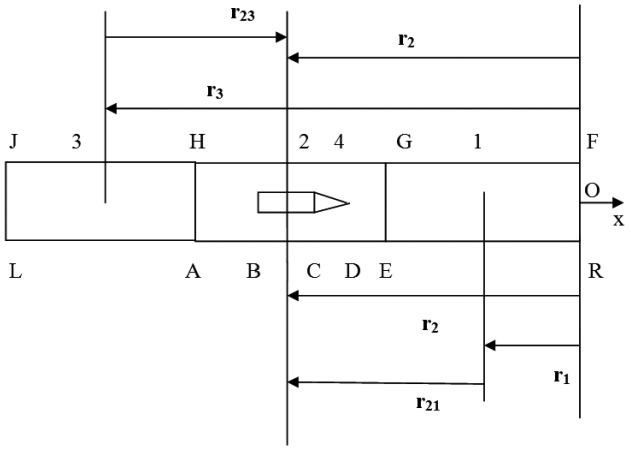

Fig. 1. We see the mercury trough AEGH and the copper "submarine", consisting of a cylindrical part (with number 2) and a right circular cone (with number 4). On the right- and on the left-hand side ends of the mercury trough, there exist two copper bar extensions of the trough (each one of length 30 cm): ERFG and LAHJ, respectively. For the calculation of the force F_{21} we consider the two current elements $\mathrm{d}l_1$ (of total length $l_1 = 0.41\,\mathrm{m} = \mathrm{DR}$ = the part with the number 1) and $\mathrm{d}l_2$ (of total length $l_2 = 0.040\,\mathrm{m} = \mathrm{BC}$). For the distance vector $\vec{r}_{21}$ between $\mathrm{d}l_1$ and $\mathrm{d}l_2$ we have: $\vec{r}_{21} = \vec{r}_2 - \vec{r}_1 = 22.5\,\mathrm{cm}\ (-\widehat{x})$, in the direction from R to A, which is the direction of motion of the copper submarine. For the force F_{23} of the part with the number 3 (that is, part LB (of length $l_3 = 0.450\,\mathrm{m}$)) on the part with the number 2 (that is, part BC of length $l_2 = 0.040\,\mathrm{m}$), we consider $\mathrm{d}l_2$ and $\mathrm{d}l_3$. For the distance vector $\vec{r}_{23}$ between $\mathrm{d}l_2$ and $\mathrm{d}l_3$ we have: $\vec{r}_{23} = \vec{r}_2 - \vec{r}_3 = 24.5\,\mathrm{cm}\ (+\widehat{x})$, in the direction opposite to that of the current I, that is, in the direction from L to A, which is the direction opposite to that of the motion of the copper submarine. We also see the common origin O of the coordinate system.

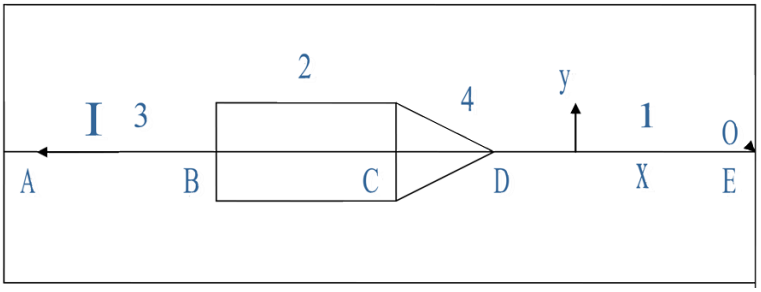

Fig. 2. Not in scale. It is shown the copper 'submarine', consisting of a short piece of straight wire squared off at one end and pointed at the other end, placed in a mercury trough 30 cm in length, with a cross-section of 0.5 inch × 0.5 inch. We see: a) part with number 2 or part CB, which is 4 cm in length and 3 mm in diameter; b) part with number 4, which is a 1 cm long taper, that is, a right circular cone, c) also part of the parts 1,3. When a current of $I = (400 \pm 8)$ A is flowing along the mercury trough the velocity of the submarine in the direction of the $-x$-axis, that is, along the current I, is $v_x = 15\,\mathrm{cm/s}$.

velocity of the submarine, v_x, by using both the B-S-G-L and Ampère force laws, is in complete agreement, within the error, with the velocity v_x experimentally measured by the experimenters.

It will be proved that the motion of the projectile (copper "submarine") in the direction of the current, with the squared off end ahead as is shown in figs. 1 and 2, in the case of the B-S-G-L force law, is due to the presence of the right circular cone (taper). The direction of the pointed end is opposite to that of the motion of the submarine. For the theoretical calculations in the case of the B-S-G-L force law we have used basic principles of Classical Electrodynamics. We obtain the magnetic induction **B** by using the Ampère law. Then we find the mechanical force of magnetic origin that exists in each elemental volume $\mathrm{d}V$, in the region of the right circular cone, where the current density **J** is immersed in the magnetic field **B**.

In [2] P. Graneau has pointed out: "For the geometry under consideration the finite-element method gives almost identical transverse force distributions with both Ampère's and the Biot-Savart-Lorentz force laws. This is remarkable in view of the different predictions the two equations make with regard to longitudinal forces".

In [3] Pappas said: "The purpose of this paper is to present the results of a very simple experiment, which favors the original Ampère force and unambiguously disproves the Biot-Savart force of relativity, or its approximation in a covariant relativistic form, namely the Lorentz force. This experiment with its extra degree of freedom has the advantage over the many other similar ones, including Ampère's original experiment, which have been performed in

the past and recently by Graneau, of giving results which are both qualitative and quantitative, as well as unambiguous. Due to the strong association of the Biot-Savart and Lorentz force to relativistic theories, the experiment can also be considered as limiting the generality of these theories".

In [4] P. Graneau also states: "An empirical law for the mechanical force between two current elements, originally deduced by Ampère from a series of classical experiments, asserts that an electric current flowing along a straight wire should place the wire in tension. All experimental evidence for non-Lorentzian longitudinal forces has been collected over a period of 160 years. Strong evidence of tensile breaks, prior to melting and evaporation of the wire, were found in an experiment [5] which has remained unexplained for eighteen years. It seems to provide proof of the existence of non-Lorentzian Ampère tension. The present letter also points out that pinch forces on the wire could conceivably produce extrusion but not tensile fracture. None of [5] photographs show the neck formation which is a feature of static tensile strength tests. When the evidence of the experiments of mine is combined with Nasilowski's findings, there remains little doubt that the observed wire fragmentation was the result of tensile fracture in the solid state of copper and aluminum wires".

The author of the present work believes that the neck formation before the wire fragmentation is the ideal case for the creation of longitudinal B-S-G-L forces.

In [6] P. Graneau says: "The Ampère electrodynamics of metallic conductors and experiments supporting it predict that the interaction of a current-carrying wire with its own magnetic field should produce longitudinal mechanical forces in the conductor, existing in addition to the transverse Lorentz forces. The longitudinal forces should stretch the conductor and have been referred to as Ampère tension. In [5] it was discovered that a current pulse would break a straight copper wire into many fragments without visible melting. A metallurgical examination of the pieces confirmed that the metal parted in the solid state. The same observation has now been made with aluminum wires. In the latest experiments the wire was bent into a semicircle and arc-connected to a capacitor discharge circuit. The arc connections ruled out rupture by Lorentz hoop tension and indicated that longitudinal forces may also arise in circular magnet windings. Explanations of wire fragmentation by thermal shock, longitudinal stress waves, Lorentz pinch-off, bending stresses, and material defects have been considered and found unconvincing. Computed Ampère tensions would be sufficient to fracture hot wires".

In [7] P. Graneau stated: "It is shown that the Ampère and Lorentz force laws to a closed current in a metallic circuit results in two different mechanical force distributions around the circuit. In addition to the transverse forces, which both laws predict, the Ampère electrodynamics requires a set of longitudinal forces that subject the conductor to tension. These longitudinal forces explain electromagnetic jet propulsion and the recoil mechanism in a railgun. Pulse current experiments are described in which Ampère tension shattered solid aluminum wires. Electrons moving through the metal lattice are the basic current-elements of the Lorentz force theory. But Ampère assumed his current-elements to be infinitely divisible. With the help of computer-aided analysis and experiment, it is demonstrated that the amperian current-element must also be of finite size and involve at least one lattice ion in addition to the conduction electron. Calculations with Ampère's formula have been found to give reasonable results when the atom, or unit atomic cell, is taken to be the smallest possible current-element. Some technological consequences of Ampère tension are discussed briefly with regard to pulse currents in normal conductors and steady currents in superconductors. The use of large macroscopic current-elements of unit length-to- width ratio gives rough approximations to the Ampère tension. The accuracy of the calculation can be improved by resolving the conductor into a number of parallel filaments, each filament being subdivided into cubic current-elements".

In [8] Carpenter pointed out: "The "Ampère tension" described by Graneau in a recent paper is due to errors in calculation and interpretation of the Ampère force law and is not a real phenomenon".

Reply by Peter Graneau: "Eighty years after the teaching of Ampère electrodynamics has ceased, because it could not deal with the motion of ions in vacuum, physicists and engineers understandably greet the revival of the old theory with disbelief. Besides, since modern electromagnetism rests on abstract ideas, as for example the free flight of energy at invariable velocity conforming with special rules of relativity, one tends to forget that an empirical law, like Ampère's, is infallible so long as it is applied to experimental situations from which it was first deduced ..."

In [9] Aspden states: "Graneau's resent interpretation of the exploding wire phenomenon as an electrodynamic effect verifying Ampère's classical formulation is questioned. Instead, it is shown that the rupturing force arising from the imbalance of the self-induced electromotive force and the ohmic potential during an explosive current surge will account for the wire breaking into several segments, as is observed".

In [10] Ternan points out: "The Lorentz and Ampère laws are shown to be equivalent. Both predict equal and opposite forces on complementary parts of a current distribution, and only a normal force on a current element. There is no force along the element. The illusory differences between the two are attributed to the incorrect integration of the differential forms of the laws, and to the inappropriate use of line current elements as sources, instead of surface or volume elements".

In [11] P. Graneau *et al.* pointed out: "This letter reports experimental results which show that electric arc currents through salt water produce explosions by electrodynamic forces rather than by the thermal expansion of gases generated in the arc column. The explosive phenomena can be explained with the aid of longitudinal Ampère forces but not with

traditional Lorentz forces. This represents the first experimental evidence indicating that Ampère's force law may be valid for dense arc plasmas".

In [12] P. Graneau states: "This communication disputes the claim made by Ternan [13] that the Ampère and Lorentz force laws are equivalent. Two examples are quoted in which the two laws make different predictions. Particle beams in vacuum obey Lorentz's law but in metallic circuits Ampère's law prevails".

In [13] Ternan stated: "The examples given by Graneau do not contradict the equivalence of the two laws in magnetostatics. Both laws give the same magnetic force per unit volume, which is normal to the current density. The stress in a conductor due to this applied force then follows from the mechanical laws of the conductor and its constraints".

In [14] Ternan claims that: "Wires that carry high currents may suffer tensile fracture. Theories for this behavior in terms of longitudinal magnetic or electric forces are refuted. The stress waves developed by rapid thermal expansion are shown to be large enough to break the wire".

In [15] Azevedo *et al.* stated: "The experiments described in this letter form a continuation of previously outlined research on electrodynamic explosions in liquids. Current pulse amplitudes have been increased from hundreds of ampere to 25 kA. The most powerful explosion so far observed imparted an impulse of 7 Ns to a metallic projectile of 1.6 kg mass. The strengths of the impulses scaled proportionally to the electrodynamic action integral. For an arbitrarily chosen current pulse shape and magnitude, the plasma explosion in saltwater is much more powerful than the action of a railgun".

In [16] P. Graneau said: "The first stage of a wire explosion is solid-state fragmentation. In [14] the author recently claimed that this is the result of rapid thermal expansion. Experimental facts are quoted in this letter which are inconsistent with the thermal explanation. Ampère tension remains to be the most likely cause of wire fragmentation. It is pointed out that the integration of Ampère's formula over a volume containing the exploding wire cancels the equal and opposite forces responsible for Ampère tension".

In [17] Dragon pointed out: "The maximum pressures developed for electric arc explosions in water range as high as 50000 atm. It was thought that these pressures were due to a sudden heating of the water to high temperatures with resulting, and equally sudden, high pressures. These are several reasons why this hypothesis is paradoxical, the main one being that temperatures of no less than 10^7 K would be required somewhere in the water arc. In this communication we discuss resent water arc explosions performed at the Massachusetts Institute of Technology. The unusual phenomena observed put these explosions in the category of experimental paradigm".

In [18] P. Graneau said: "In this paper the mechanical efficiency of the railgun is defined as the force accelerating the armature-projectile combination divided by the total electrodynamic force generated in the gun. The energy expended in a shot may then be equated to the ohmic loss plus the kinetic energy that would have been developed in the absence of mechanical losses. In this way it can be shown that the overall energy efficiency can never be greater than the square of the mechanical efficiency. Comparing calculations with experimental data makes it clear the reported disappointing performance of railguns is due to some ill-understood mechanical deficiency. A simple experiment is described which reveals buckling and distortion of the rails by recoil action. This explains the mechanical inefficiency. In relativistic electromagnetism, the recoil force should act "on the magnetic field" and absorb field-energy momentum. The Ampère-Neumann electrodynamics, on the other hand, requires the recoil forces to reside in the railheads and push the rails back toward the gun breech. Experiment confirmed the latter mechanism".

In [19] Peoglos said: "The results are reported of an experiment designed to measure the force exerted by a current circuit on a part of itself and to compare this to the predictions of the Biot-Savart and Ampère magnetostatic force laws. The design of the experiment was such as to limit the current through the circuits to values below about 1 A, to optimize the removal of the heat generated in the conductors and to minimize the magnetohydrodynamic and other effects in the mercury at the contact points between the two sections of the circuits. Contrary to previously reported results, agreement between experiment and theory is found, within 1 to 2%, which is the limit set by experimental uncertainties".

In [20] Christodoulides pointed out: "The force laws of Ampère and Biot-Savart in magnetostatics are compared using the geometrical model of a closed curve to represent a current loop. The two laws give identical results when forces between separate current loops are considered and also for the force exerted by a current loop on a rectilinear part of itself. According to both laws, these self-forces diverge whenever the curvature of the curve representing the current loop is not equal to zero. Differences in the predictions of the two laws are shown only as differences in diverging forces when evaluating forces of a current loop on a part of itself and to be entirely due to the oversimplified and unrealistic geometrical model used for the current loop".

In [21] Nasilowski says: "This letter argues that Ampère and Graneau are correct in explaining Ampère's hairpin experiment by the longitudinal forces contained in Ampère's force law".

In [22] P. Graneau stated: "The cause of thunder is one of the oldest riddles of recorded scientific speculation. Three centuries BC Aristotle published the first thunder theory. Many other theories were proposed until at the beginning of the present century a consensus evolved which assumed thunder must begin with a shockwave in air due to the sudden thermal expansion of the plasma in the lightning channel. The only experimental support for

this theory came from spectroscopic temperature determinations up to 36000 K. Any one of the assumptions made in equating "optical" to thermodynamic temperatures can be challenged and some have been disputed. Experiments with short atmospheric arcs of lightning strength revealed average arc pressures in excess of 400 atm and peak pressures approaching 1000 atm. These results demand much higher temperatures than those found by lightning spectroscopy. Furthermore, when the strength of the short arc explosions was plotted against the action integral of the current pulse it followed an electrodynamic law rather than a heating curve. Arc photography then proved conclusively that the plasma did not expand thermally in all directions, but preferentially at right angles to the current, as if driven by organized electrodynamic action. Possible electrodynamic forces which might drive the thunder shockwave are the Lorentz pinch force, the longitudinal Ampère force, and the alpha-torque force of the Ampère-Neumann electrodynamics. The pinch force was found to be far too small and in the wrong direction to be the cause of thunder. Longitudinal and alpha-torque forces act in the correct direction but, so far, quantitative agreement has not been achieved. This may have to wait for a complete Ampère MHD".

In [23] P. Graneau mentioned: "MHD ship propulsion has now been researched for ten years. In the conventional method a strong superconducting magnet is installed on the ship and electrolytic dc current is driven through the seawater across the magnetic lines of flux. The seawater jet engine discussed in this paper differs from standard MHD propulsion in that it does not employ a magnet, but relies on the Ampère forces of reaction between solid (electrode) and liquid (seawater) current elements. The jet propulsion force is proportional to the square of the current. In order to permit the flow of sufficiently large electronic currents, the salt-water has to be broken down and converted to a water-arc plasma".

In [24] Phipps *et al.* said: An experiment proposed by Wesley involving passing current through a mercury cell of varying cross section has been performed and appears to confirm the existence of Ampère tension (Ampère longitudinal forces). Ampère's force law predicts longitudinal forces of repulsion between collinear current elements, whereas Lorentz' s force law predicts none.

In [25] Rambaut said: "The Ampère-Weber potential associated with the Ampère forces recently experimentally established between current elements is shown to be deductible, as non-relativistic approximation, from the sum of a particular relativistic representation of the Lienart-Wiechert four-vector potentials acting on a mixture of extended, individual positively and negatively charged particle source components. Some consequences on the physical stability of e.m. currents both in solids, liquids and plasmas (tokamak) are briefly discussed".

In [26] Rambaut said: "In the light of the subsequent discovery of atoms and electrons, the empirical current — current interactions discovered by Ampère in 1820 evidently reflect a very simplified model of the collective behavior of the complex randomly agitated charged current constitutive components individually by the Maxwell-Lorentz-Einstein electromagnetic laws. It is shown here that the approximate empirically rediscovered Ampère-Weber laws (justified by Rambaut and Vigier) can also be directly derived from a spherical Fermi distribution of interacting charged particles, tied to a surprisingly simple model of ion-electron interacting couples constituting current elements".

In [27] Rambaut said: "An experiment performed in Kiel in 1973 paves the way to a possible new model of non-thermonuclear fusion. The process could be pycnonuclear and explain other experiments such as the Z-pinch and cluster fusion. The proposed fusion mechanism is based on quantum tunneling combined with the screening of the Coulomb barrier of two colliding deuterons by electron clouding favoured by chaos. Possible break-even conditions by this mechanism are discussed".

In [28] Rambaut mentioned: "In a dense, fully ionized medium, containing fusible nuclei, a collision between two nuclei is accompanied by an electron concentration around them. By this, rate of tunneling is tremendously increased. The experimental results are in agreement with the calculations, the number of displaced electrons being typically in the range of one to two thousand".

In [29] P. Graneau *et al.* stated: "Three different non-tokamak fusion mechanisms are examined, involving plasma filaments formed from gaseous, liquid or solid deuterium. Results from previous experiments, in which up to 10^{12} neutrons were produced, point to non-thermal fusion mechanism. The role of electrodynamic forces, including those predicted by Ampère's force law, are investigated as the possible mechanism of ion acceleration". "There is no doubt that pinch forces are responsible for the formation of the plasma filament, but we are faced with two possible rupture mechanisms. Without knowledge of longitudinal Ampère forces, investigators had no choice but to attribute filament rupture to an $m = 0$ MHD instability. This phenomenon forms a neck in the filament, and the consequent radial current components on both sides of the neck repel each other and fracture the plasma column. Using the Ampère electrodynamics, we expect the longitudinal repulsion of current elements (deuterons) to be the cause of the fracture, with no requirement for the formation of a neck. In both cases the electron current continues to flow across the gap without producing a visible plasma".

The author of the present work believes that the formation of a neck in the filament is the ideal case for the subsequent creation of longitudinal B-S-G-L forces.

In [30] P. Graneau *et al.* pointed out: "Recent developments in filamentary fusion techniques are discussed. Ampère's electrodynamic force law is used to calculate the forces on filamentary currents, and is shown to predict the observed

beading. Subsequent computation reveals compression forces on the beads, which may be sufficient to account for the observed fusion reactions".

In [31] N. Graneau stated: "The role of electrodynamic theory in vacuum arc processes has long been recognized in some aspects of modern theory and design of vacuum interrupters, and almost completely ignored in others. For example, it is well known that the motion of cathode spots is of electromagnetic origin, thus leading to methods of steering the spots by controlling the direction of the self and applied magnetic fields. However, the work presented here primarily involves the ion flux from the cathode spot. There are two well-recognized features of this flux that are very striking, and both have proved to be difficult to explain. These are the anomalously high energies of the ions, and their highly anisotropic spatial distribution. An electrodynamic acceleration mechanism based on Ampère's force law is proposed as an explanation to these phenomena. This theory is shown to be consistent with existing particle production models, and also provides a consistent solution to macroparticle emission and retrograde motion".

In [32] P. Graneau *et al.* pointed out: "This letter discusses the failure of the Lorentz force law to locate the recoil action in railguns. Ampère's force law makes predictions which agree with experiment".

In [33] Cavalleri *et al.* said: The results of measurements of the force on a part of a circuit carrying a steady current, due to the action of the whole current loop, are reported. The theoretical value of the force has been calculated using the standard electrodynamics force law. Taking into account the finite dimension of the wire forming the current loop, the calculation implies the computation of a sixfold integral. Contrary to the past experimental outcome reported in the literature [3,24], a comparison of a theoretical prediction with the present experimental results corroborates the standard force law within the limits of experimental errors.

In [34] Cavalleri *et al.* said: "Our paper [33] described experimental results that brought into agreement standard theory and experiment, in contrast to two previous experiments that claimed disagreement [3,24]. The shape of our circuit was designed to improve knowledge of the electric flux lines. Such a shape required numerical calculations to predict the relevant force on the mobile part of the circuit".

In [35] N. Graneau *et al.* said: According to the conventional views of electromagnetic theory, as these are expressed in the Lorentz force law, all the forces which act on a current metallic conductor are perpendicular to the current streamlines. However, over the years, from Ampère through Maxwell until the present day, there have been persistent claims that when current flows in a metallic conductor, there are mechanical forces acting along current streamlines which subject the conductor to tensile stress, and which are therefore capable of performing work in the direction of current flow. The problem of substantiating these claims has always lain in the difficulty of designing an experiment in which the effects are unambiguously demonstrated. The present paper describes an experiment which to a large extent removes these ambiguities, and which provides a compelling novel demonstration of forces acting along current streamlines. A force calculation based on Ampère's original electrodynamic force law is found to be consistent with the observed behavior.

In [36] P. Graneau and N. Graneau pointed out: Cavalleri *et al.* [33] have attempted to resolve the electrodynamic force law controversy. This attempt to prove the validity of either the Ampère or Lorentz force law by theory and experiment has revealed only that the two are equivalent when predicting the force on part of a circuit due to the current in the complete circuit. However, in our analysis of internal stresses, only Ampère's force law agrees with experiment.

In [37] Cavalleri *et al.* said: Our paper [33] confirmed the validity of both Ampère and Grassmann's force law even for the action exerted on a part of a current loop. Since that part can be an element of a circuit, both force laws also predict the same internal stresses and the same recoil for a railgun. Graneau and Graneau (preceding paper [36]) neglected the action on the breech of the railgun, an action that produces the same recoil for both force laws. The reaction to the force exerted on the armature does not act on the rails but on the breech that, simply because of symmetry, undergoes a force equal and opposite to the one acting on the armature. P. Graneau implicitly in [36] and explicitly in [12] states that experiments favor the Lorentz force law in electron guns (*i.e.* on free electrons) and Ampère's force law on current elements. This statement has been proved wrong by Cavalleri *et al.* [38].

In [38] Cavalleri *et al.* said: An experiment of impulsive electrodynamics [35] has been interpreted by the experimenters as a confirmation of Ampère's law, because they consider the force exerted on a mobile section as due only to another small section. The integration over all the circuit gives zero longitudinal force by both Ampère's and Grassmann's laws. The correct interpretation of the experiment comes from analyzing the contributions of the different air pressures in the two air gaps due to different solid angles for radiation and particle losses during the electrical discharge. Moreover, there is a larger number of ions hitting the bases of the smaller gap because of a larger useful solid angle. Finally, ions are more trapped in the smaller gap because of a larger number of bounces. This interpretation leads to a better agreement with the experimental results. The longitudinal forces observed in ref. [35] must therefore have another interpretation. We prove that it is not possible to state that experiments favor Lorentz force law for free electrons and Ampère force law for current elements.

In [39] Ajoy said: The self-force experienced by a semicircular conducting loop of circular cross section is evaluated analytically using the Lorentz force expression and shown to agree with the result of the partially analytical and partially numerical calculations quoted in the paper of Cavalleri *et al.* [33].

In [40] Cavalleri *et al.* said: The results of an experiment of impulsive electrodynamics [40] are shown to be due to electrons and ions in run-aways. By fitting the theoretical values with the experimental data, the values of microscopic quantities, at present unknown, can be derived, thus opening a new field of research. The obtained quantities are three, namely: i) the contribution to air ionization due to the current (mainly of run-aways) and characterized by a parameter ρ; ii) the product $\zeta = n_{\rm ei} \cdot n_{\rm ie}$ (where $n_{\rm ei}$ is the number of ions extracted by one electron in run-away and $n_{\rm ie}$ the number of electrons extracted one run-away ion colliding on the electrodes in electrical discharges with temperatures (for non run-aways) of $\cong 4 \cdot 10^4\,{\rm K}$); iii) the reconstruction time constant T of the high-energy tail of the distribution function, from which we can derive the concentration per unit time of electrons and ions which become run-aways. The T value is useful for the theoretical explanation of the electronic noise with power spectral density inversely proportional to the frequency.

The author of [1] in his work has not given any data for the accuracy with which he has measured the electric current of 400 A. Also, he has not given the experimental error in the measurement of the projectile's velocity: $\upsilon_x = 15\,{\rm cm/sec}$. So, we have to guess and apply certain calculated errors for the quantities involved in his experiment.

All calculations were done using MATLAB (R2011a) of N.T.U.A.

The structure of our paper is the following. In sect. 2 we give the form of the Ampère and Biot-Savart-Grassmann-Lorentz force laws using volume elements and current densities. In sect. 3 we reveal the mechanism for the creation of longitudinal forces by the B-S-G-L force law. In sect. 4 we give the drag force. In sect. 5 we present the calculation of the velocity υ_x, along the x-axis, according to the Biot-Savart-Grassmann-Lorentz force law. In sect. 6 we show the calculation of the longitudinal forces according to the Ampère's force law. In sect. 7 we present the calculation of the velocity according to the Ampère force law. In sect. 8 we find the longitudinal Ampère and B-S-G-L forces in the case both ends of the wire are squared off. In sect. 9 we present the conclusion.

2 The form of the Ampère and Biot-Savart-Grassmann-Lorentz force laws using volume elements and current densities

The electrodynamic force law–equation of Ampère between an electrical current element 1 and another current element 2 was discovered in 1823 [41]. Including sixfold integrals, volume elements and current densities, this law has the form [42]

$$\mathrm{d}^6 F_{fi} = \frac{\mu_0}{4\pi} J_i \cdot J_f \cdot \left(-\frac{\vec{r}_{fi}}{{r_{fi}}^3}\right) \cdot \left[2 \cdot \mathrm{d}\vec{l_i} \cdot \mathrm{d}\vec{l_f} - \frac{3}{{r_{fi}}^2}\left(\mathrm{d}\vec{l_i} \cdot \vec{r}_{fi}\right)\left(\mathrm{d}\vec{l_f} \cdot \vec{r}_{fi}\right)\right] \cdot \mathrm{d}A_i \cdot \mathrm{d}A_f, \tag{1}$$

where $\vec{r}_{fi} = \vec{r}_f - \vec{r}_i$.

In the above equation $\mathrm{d}A_i$ and $\mathrm{d}\vec{l_i}$ are the cross-sectional area and the length of the volume element $\mathrm{d}V_i$, while $\vec{r}_f$ and $\vec{r}_i$ are the vector distances of $\mathrm{d}V_f$ and $\mathrm{d}V_i$ from a common origin of coordinates. $\vec{r}_{fi}$ is the distance between the two volume elements, $\mathrm{d}^6\vec{F}_{fi}$ is the differential force acting on element $\mathrm{d}V_f$, in which there is a current density $\vec{J}_f$, due to the current in element $\mathrm{d}V_i$. The element $\mathrm{d}\vec{l_i}$ has the direction of the current density $\vec{J}_i$ and is always perpendicular to the area $\mathrm{d}A_i$. J is taken as $I/$ (cross-sectional area of the wire), where I is the current in the wire.

Biot and Savart first proposed in 1820 the magnitude of the magnetic induction due to a small current element [43]. Grassmann and, in 1831, Michael Faraday, discovered that when a wire currying a current is placed in the field of a magnet a mechanical force is exerted on the wire. Lorentz A. Hendric, towards the end of the decade of 1890, formulated the electrodynamic Lorentz force law including the charge and its velocity, that is, the B-S-G-L force law.

In its final form the Biot-Savart-Grassmann-Lorentz force law between an electrical current element 1 and another current element 2 is [44,45]

$$\mathrm{d}^6 F_{fi} = \frac{\mu_0}{4\pi} J_i J_f \frac{\mathrm{d}\vec{l_f} \times \left[\mathrm{d}\vec{l_i} \times \vec{r}_{fi}\right] \mathrm{d}A_i \mathrm{d}A_f}{{r_{fi}}^3}. \tag{2}$$

3 The mechanism for the creation of longitudinal forces by the B-S-G-L force law

3.1 The magnetic field in the right circular cone

3.1.1

From the data in [1] we find that the magnitude of the current density $\vec{J}$ through the cross-sectional area of the mercury trough, which is $0.5 \times 0.5\,{\rm inch}^2$, has the value

$$J = \frac{I}{A} = \frac{I}{l^2} = \frac{400\,{\rm A}}{[0.5 \cdot 2.5\,{\rm cm}] \cdot [0.5 \cdot 2.5\,{\rm cm}] \cdot [10^{-4}]} = (2560000)\frac{A}{m^2}, \tag{3}$$

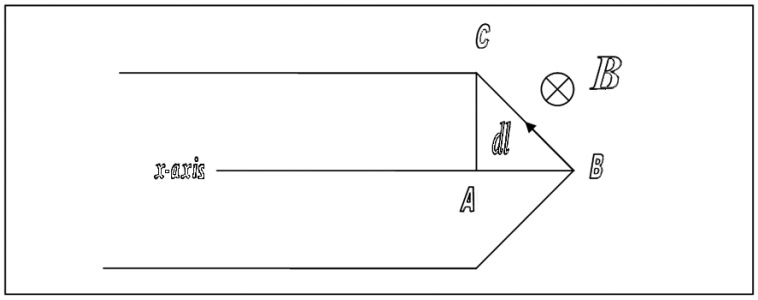

Fig. 3. We see part of the copper submarine showing the pointed end, that is, the right circular cone. $AB = 10\,\mathrm{mm}$, $AC = 1.5\,\mathrm{mm}$. We also show: a) the direction of the magnetic field B above the line AB; b) the direction of the current element $\mathrm{d}\vec{l}$; and c) the direction of the $-x$-axis, that is in the direction of the motion of the copper submarine.

where $l^2 = [1.25 \cdot 10^{-2}]^2\,\mathrm{m}^2$, with $l \pm \sigma l = [1.25 \cdot 10^{-2} \pm 0.001]\,\mathrm{m}$, is the cross-section of the mercury trough. We have

$$\sigma(J) = \sqrt{\left(\frac{\partial J}{\partial I}\right)^2 \sigma^2(I) + \left(\frac{\partial J}{\partial l}\right)^2 \sigma^2(l)} = \sqrt{\left(\frac{1}{l^2}\right)^2 \sigma^2(I) + \left(\frac{I \cdot 2 \cdot l}{l^4}\right)^2 \sigma^2(l)}$$
$$= \sqrt{2.6214 \cdot 10^9 + 1.6777 \cdot 10^{11}}\,\mathrm{A/m^2} = 412790\,\mathrm{A/m^2}. \tag{4}$$

Thus, $J \pm \sigma J = [2560000 \pm 412790]\,\mathrm{A/m^2}$.

3.1.2

In a solid cylindrical conductor with base radius R, having a steady current I distributed uniformly over its cross-section, the current density is $J = I/\pi R^2$. Inside the cylinder Ampère's law, $\oint \vec{B} \cdot \mathrm{d}\vec{l} = \mu_0 \iint \vec{J} \cdot \mathrm{d}\vec{A}$, tells us that the magnetic field B is determined solely by the current flowing inside a circle of radius r (where $r \leq R$) and is given by

$$B = \frac{\mu_0 J r}{2} = \frac{\mu_0 I}{2\pi R^2} r (r \leq R). \tag{5}$$

It should be pointed out that Ampère's law is valid for steady currents and is approximately valid for slowly varying currents. In free space and inside conducting nonmagnetic materials, such us copper, the permeability μ is approximately that of free space [μ_0], that is, $\mu = \mu_0$.

3.2 The mechanical force of magnetic origin that moves the projectile

The mechanical force of magnetic origin that exists in each elemental volume $\mathrm{d}V_{\mathrm{vol}}$ is given by

$$\mathrm{d}\vec{F}_{\mathrm{mech}} = \vec{J} \times \vec{B} \mathrm{d}V_{\mathrm{vol}}. \tag{6}$$

This mechanical force, eq. (6), in the region of the right circular cone (the pointed end of the "submarine" in figs. 1 and 2), where the current density $\vec{J}$ is immersed in the magnetic field $\vec{B}$, takes the form, considering that $J = I/A$ and also that $J(\mathrm{d}V) = J(\mathrm{d}l)(\mathrm{d}A)$,

$$\mathrm{d}\vec{F}_{\mathrm{mech}} = \oint I \cdot \mathrm{d}\vec{l} \times \vec{B} = \oint I \cdot \left(\mathrm{d}\vec{l_x} + \mathrm{d}\vec{l_y}\right) \times \vec{B} = \oint I \cdot \mathrm{d}\vec{l_y} \times \vec{B}, \tag{7}$$

since for the current element $\mathrm{d}\vec{l}$ we have $\mathrm{d}\vec{l} = \mathrm{d}\vec{l_x} + \mathrm{d}\vec{l_y}$.

The direction of the current element $\mathrm{d}\vec{l_x}$ is along the direction of the $-x$-axis, that is, the direction DA in fig. 2 or the direction BA in fig. 3, while the direction of the current element $\mathrm{d}\vec{l_y}$ is normal to $\mathrm{d}\vec{l_x}$. The magnitude of the magnetic field **B** on the x-axis, the axis of the cone, is zero.

Considering eqs. (5), (6) and (7), and also that the differential $\mathrm{d}l_y$ (see fig. 4) corresponds to the differential $\mathrm{d}r$, where r is the radius in eq. (5), we find, for the mechanical force of magnetic origin along the $-x$-axis,

$$\mathrm{d}F_{\mathrm{mech}} = I \mathrm{d}l_y B = I \mathrm{d}r \frac{\mu_0 J r}{2} = \frac{I \mu_0 J}{2} r \mathrm{d}r. \tag{8}$$

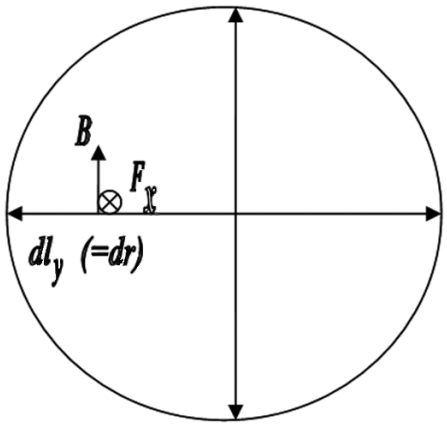

Fig. 4. We show a cross-section, which is perpendicular to the $-x$-axis (the direction of the current flow) in the region of the 1 cm long taper (the right circular cone, that is, the right pointed end of the copper submarine). We see: a) the direction of the current element $\mathrm{d}l_y$ which corresponds to $\mathrm{d}r$; b) the direction of the magnetic field $\mathbf{B}$; and c) the direction of the $-x$ component of the Biot-Savart-Faraday-Lorentz force, F_x, that is parallel to the $-x$-axis. The force F_x is along the direction of the motion of the copper submarine which is normal to the page.

With $\mu_0 = 4\pi \times 10^{-7}\,\mathrm{Tm/A}$ we find, for this mechanical force along the $-x$-axis,

$$F_{\mathrm{mech}} = \frac{I\mu_0 J}{2}\left.\frac{r^2}{2}\right|_0^{1.5\,\mathrm{mm}} = 400(\mathrm{A})\cdot 4\pi\cdot 10^{-7}(T\cdot\,\mathrm{m/A})\cdot 2560000(\,\mathrm{A/m^2})\cdot(1.5\cdot 10^{-3})^2(\,\mathrm{m^2})\cdot\frac{1}{4} = 7.2382\cdot 10^{-4}N. \quad (9)$$

We have

$$\sigma(F_{\mathrm{mech}}) = \sqrt{\left(\frac{\partial F_{\mathrm{mech}}}{\partial I}\right)^2\sigma^2(I) + \left(\frac{\partial F_{\mathrm{mech}}}{\partial J}\right)^2\sigma^2(J)} = \sqrt{\left(\frac{J\cdot\mu_0\cdot r^2}{4}\right)^2\sigma^2(I) + \left(\frac{I\cdot\mu_0\cdot r^2}{4}\right)^2\sigma^2(J)} = 1.1761\cdot 10^{-4}N \quad (10)$$

and

$$F_{\mathrm{mech}} \pm \sigma(F_{\mathrm{mech}}) = (7.24 \pm 1.18)\cdot 10^{-4}N. \quad (11)$$

4 The drag force

The sign of the drag force is negative because it opposes to the vehicle's motion, which in our case is along the $-x$-axis. A symmetric streamlined body at zero angle of attack experiences only a drag force, that has the form

$$F_{\text{Drag-force}} = -\frac{1}{2}\rho C_A A_0 \upsilon^2\,, \quad (12)$$

where ρ is the mass density of the fluid (in our case mercury, $\rho_{\mathrm{Hg}} = 13.546\,\mathrm{gr/cm^3} = 13545.7\,\mathrm{kg/m^3}$); υ is the speed of the object relative to the fluid, which in our case is along the $-x$-axis ($= \upsilon_x$); A_0 is the characteristic frontal area of the body, that is, the moving shape $= \pi\cdot R^2 = \pi\cdot(1.5\,\mathrm{mm})^2$. C_A (the subscript A denotes zero angle of attack conditions) is the drag coefficient, which is 0.82 for long cylinder, 1.15 for short cylinder and 0.50 for cone (see `http://en.wikipedia.org/wiki/Drag_coefficient`). We take $C_A = 0.90 \pm 0.40$, considering an absolute error of 0.40 in C_A.

Thus, we have

$$F_{\text{Drag-force}} = -\frac{1}{2}\cdot 13545.7\cdot 0.9\cdot\pi\cdot(1.5\cdot 10^{-3})^2\cdot\upsilon_x^2 = -0.0431\cdot\upsilon_x^2(N). \quad (13)$$

5 Calculation of the velocity υ_x, along the x-axis, according to the B-S-G-L force law

The drag force, $F_{\text{Drag-force}}$, should be equal and opposite to the mechanical force of magnetic origin, F_{mech}, along the x-axis. For the modulus, we have $F_{\text{Drag-force}} = F_{\mathrm{mech}}$, or

$$0.5\cdot\rho\cdot C_A\cdot A_0\cdot {\upsilon_x}^2 = F_{\mathrm{mech}} = 7.2382\cdot 10^{-4}N. \quad (14)$$

Solving for v_x, the modulus of the velocity v along the x-direction, we obtain

$$v_x = \sqrt{\frac{F_{\rm mech}}{0.5\rho C_A A_0}} = \sqrt{\frac{7.2382\cdot 10^{-4}N}{0.5\cdot 13545.7(\,{\rm kg/m^3})(0.90)\pi(1.5\cdot 10^{-3})^2\,{\rm m^2}}} = 0.1296(\,{\rm m/s}). \tag{15}$$

From eqs. (14) and (15), we have

$$\begin{aligned}\sigma({v_x}^2) &= \sqrt{\left(\frac{\partial {v_\chi}^2}{\partial F_{\rm mech}}\right)^2\sigma^2(F_{\rm mech}) + \left(\frac{\partial {v_{\chi^2}}}{\partial C_A}\right)^2\sigma^2(C_A) + \left(\frac{\partial {v_\chi}^2}{\partial R}\right)^2\sigma^2(R)}\\ &= \sqrt{X_1+X_2+X_3} = 0.0083\,{\rm m^2/s^2} \quad \text{and} \quad \sigma(v_x) = 0.091\,{\rm m/s},\end{aligned}$$

where

$$\begin{aligned}X_1 &= \left(\frac{1}{(0.5\rho C_A\pi R^2)}\right)^2\sigma^2(F_{\rm mech})\\ &= \left(\frac{1}{[0.5\cdot 13545.7\cdot 0.9\cdot\pi\cdot(1.5\cdot 10^{-3})^2]}\right)^2(1.1761\cdot 10^{-4})^2\\ &= 7.4507\cdot 10^{-6}\,{\rm m^4/s^4}\\ X_2 &= \left(\frac{F_{\rm mech}0.5\rho\pi R^2}{(0.5\rho C_A\pi R^2)^2}\right)^2\sigma^2(C_A)\\ &= \left(\frac{7.23829\cdot 10^{-4}\cdot 0.5\cdot 13545.7\cdot\pi\cdot(1.5\cdot 10^{-3})^2}{[0.5\cdot 13545.7\cdot\pi\cdot(1.5\cdot 10^{-3})^2(0.90)]^2}\right)^2(0.40)^2\\ &= 5.5746\cdot 10^{-6}\,{\rm m^4/s^4}\\ X_3 &= \left(\frac{F_{\rm mech}(2\pi R)0.5\rho C_A}{(0.5\rho C_A\pi R^2)^2}\right)^2\sigma^2(R)\\ &= \left(\frac{7.23823\cdot 10^{-4}\cdot 0.5\cdot 13545.7\cdot 2\pi\cdot(1.5\cdot 10^{-3})(0.9)}{[0.5\cdot 13545.7\cdot(0.9)\pi\cdot(1.5\cdot 10^{-3})^2]^2}\right)^2[(0.1\cdot 10^{-3})]^2\\ &= 5.0171\cdot 10^{-6}\,{\rm m^4/s^4}\end{aligned} \tag{16}$$

Thus we obtain, using the B-S-G-L force law,

$$v_x \pm \sigma(v_x) = (0.13\pm 0.09)\,{\rm m/s}. \tag{17}$$

6 Calculation of the longitudinal forces according to the Ampère force law

In the case of the Ampère force law, eq. (1), four forces are involved: $\vec{F}_{21}, \vec{F}_{23}, \vec{F}_{41}$ and $\vec{F}_{43}$. We calculate all four forces with respect to a common origin O (see figs. 1 and 2) of a coordinate system. O is located at the most right point of the right-hand side copper extension of the trough (see fig. 1). We find what follows.

6.1

For the force F_{21} of the part with the number 1 (that is part DR of length $l_1\pm\sigma l_1 = [0.41(=0.30+0.10+0.01)\pm 0.001]\,{\rm m}$) on the part with the number 2 (that is part BC of length $(l_2\pm\sigma l_2 = (0.040\pm 0.001)\,{\rm m})$), as can be seen in fig. 1, we consider the two current elements ${\rm d}n$ (with the number $1 = {\rm d}l_1$) and ${\rm d}m$ (with the number $2 = {\rm d}l_2$) centred at the centre of the parts of 4 cm (BC) and 41 cm (DR), respectively. For the distance vector $\vec{r}_{mn} = \vec{r}_{21}$ between the two current elements ${\rm d}n$ and ${\rm d}m$ we have $\vec{r}_1 = [(30+10+1)/2]\,{\rm cm}(-\widehat{x}) = 20.5\,{\rm cm}(-\widehat{x})$, $\vec{r}_2 = (30\,{\rm cm}+10\,{\rm cm}+3\,{\rm cm})(-\widehat{x}) = 43\,{\rm cm}(-\widehat{x})$ and $\vec{r}_{mn} = \vec{r}_{21} = \vec{r}_2 - \vec{r}_1 = [43\,{\rm cm} - 20.5\,{\rm cm}](-\widehat{x}) = 22.5\,{\rm cm}(-\widehat{x})$, with $r_{21}\pm\sigma(r_{21}) = [0.225\pm 0.001]\,{\rm m}$, in the direction of the current I (that is, in the direction from R to A in fig. 1), which is the direction of motion of the copper submarine.

Using eq. (1) we find

$$\begin{aligned}
&\mathrm{d}^2\vec{F}_{21} = -\frac{\mu_0}{4\pi} I_1 \cdot I_2 \frac{\widehat{r}_{21}}{{r_{21}}^2}\left[2\mathrm{d}\vec{l}_1 \cdot \mathrm{d}\vec{l}_2 - \frac{3}{{r_{21}}^2}(\mathrm{d}\vec{l}_1 \cdot \vec{r}_{21})(\mathrm{d}\vec{l}_2 \cdot \vec{r}_{21})\right] \\
&\Rightarrow \vec{F}_{21} = -\frac{\mu_0}{4\pi} I_1 I_2 \frac{(-\widehat{x})}{{r_{21}}^2}\left[2\int_{-0.02}^{0.02} \mathrm{d}l_1(-\widehat{x}) \cdot \int_{-0.205}^{0.205} \mathrm{d}l_2(-\widehat{x}) - 3\int_{-0.02}^{0.02} \mathrm{d}l_1(-\widehat{x}) \cdot (-\widehat{x}) \int_{-0.205}^{0.205} \mathrm{d}l_2(-\widehat{x}) \cdot (-\widehat{x})\right] \\
&\qquad = -\frac{\mu_0}{4\pi} I_1 I_2 \frac{(-\widehat{x})}{{r_{21}}^2}\left[2\int_{-0.02}^{0.02} \mathrm{d}l_1 \int_{-0.205}^{0.205} \mathrm{d}l_2 - 3\int_{-0.02}^{0.02} \mathrm{d}l_1 \int_{-0.205}^{0.205} \mathrm{d}l_2\right] \\
&\Rightarrow \vec{F}_{21} = \widehat{x}\frac{10^{-7} \cdot 400 \cdot 400}{0.225^2}[2 \cdot 0.04 \cdot 0.41 - 3 \cdot 0.04 \cdot 0.41] = -\widehat{x}0.0051832\ N,
\end{aligned} \tag{18}$$

where $\widehat{x}$ is the unit vector along the direction x.

We have

$$\sigma(F_{21}) = \left(\left(\frac{\partial F_{21}}{\partial I_1}\right)^2 \sigma^2(I_1) + \left(\frac{\partial F_{21}}{\partial I_2}\right)^2 \sigma^2(I_2) + \left(\frac{\partial F_{21}}{\partial r_{21}}\right)^2 \sigma^2(r_{21})\right)^{1/2} = 1.5367 \cdot 10^{-4} N.$$

So,

$$\vec{F}_{21} \pm \sigma(F_{21}) = -\widehat{x}(51.832 \pm 1.537) \cdot 10^{-4} N. \tag{19}$$

6.2

For the force F_{23} of the part with the number 3 (that is, part LB (of length $l_3 \pm \sigma l_3 = (0.300 + 0.150) \pm 0.001\,\mathrm{m} = (0.450) \pm 0.001)\,\mathrm{m}$) on the part with number 2 (that is, part BC (of length $l_2 \pm \sigma l_2 = (0.040 \pm 0.001)\,\mathrm{m}$)), as can be seen in fig. 1, we consider the two current elements $\mathrm{d}m$ (with number $2 = \mathrm{d}l_2$) and $\mathrm{d}n$ (with number $3 = \mathrm{d}l_3$) centred at the centre of the parts of 4 cm (BC) and 45 cm (LB), respectively.

For the distance vector $\vec{r}_{mn} = \vec{r}_{23}$ between the two current elements $\mathrm{d}n$ and $\mathrm{d}m$ we have $\vec{r}_2 = [(30 + 10 + 3)]\,\mathrm{cm}(-\widehat{x}) = 43\,\mathrm{cm}(-\widehat{x})$, $\vec{r}_3 = (30\,\mathrm{cm} + 10\,\mathrm{cm} + 5\,\mathrm{cm} + 15\,\mathrm{cm} + 7.5\,\mathrm{cm})(-\widehat{x}) = 67.5\,\mathrm{cm}(-\widehat{x})$ and $\vec{r}_{mn} = \vec{r}_{23} = \vec{r}_2 - \vec{r}_3 = [43\,\mathrm{cm} - 67.5\,\mathrm{cm}](-\widehat{x}) = 24.5\,\mathrm{cm}(+\widehat{x})$, with $r_{23} \pm \sigma(r_{23}) = [0.245 \pm 0.001]\,\mathrm{m}$, in the direction opposite to that of the current I, that is, in the direction from L to A in fig. 1, which is the direction opposite to that of the motion of the copper submarine.

From eq. (1) we obtain

$$\begin{aligned}
&\mathrm{d}^2\vec{F}_{23} = -\frac{\mu_0}{4\pi} I_2 \cdot I_3 \frac{\widehat{r}_{23}}{{r_{23}}^2}\left[2\mathrm{d}\vec{l}_2 \cdot \mathrm{d}\vec{l}_3 - \frac{3}{{r_{23}}^2}(\mathrm{d}\vec{l}_2 \cdot \vec{r}_{23})(\mathrm{d}\vec{l}_3 \cdot \vec{r}_{23})\right] \\
&\Rightarrow \vec{F}_{23} = -\frac{\mu_0}{4\pi} I_2 \cdot I_3 \frac{\widehat{x}}{{r_{23}}^2}\left[2\int_{-0.02}^{0.02} (-\widehat{x}\,\mathrm{d}l_2) \cdot (-\widehat{x}) \int_{-0.225}^{0.225} \mathrm{d}l_3 - 3\int_{-0.02}^{0.02} (-\widehat{x}\,\mathrm{d}l_2) \cdot (+\widehat{x}) \int_{-0.225}^{0.225} (-\widehat{x}\,\mathrm{d}l_3) \cdot (\widehat{x})\right] \\
&\qquad = -\frac{\mu_0}{4\pi} I_2 \cdot I_3 \frac{\widehat{x}}{{r_{23}}^2}\left[2\int_{-0.02}^{0.02} \mathrm{d}l_2 \int_{-0.225}^{0.225} \mathrm{d}l_3 - 3\int_{-0.02}^{0.02} \mathrm{d}l_2 \int_{-0.225}^{0.225} \mathrm{d}l_3\right] \\
&\qquad = -\widehat{x}\frac{10^{-7} \cdot 400 \cdot 400}{0.245^2}[2 \cdot 0.04 \cdot 0.45 - 3 \cdot 0.04 \cdot 0.45] = \widehat{x}0.004789N.
\end{aligned} \tag{20}$$

We have

$$\sigma(F_{23}) = \left(\left(\frac{\partial F_{23}}{\partial I_2}\right)^2 \sigma^2(I_2) + \left(\frac{\partial F_{23}}{\partial I_3}\right)^2 \sigma^2(I_3) + \left(\frac{\partial F_{23}}{\partial r_{23}}\right)^2 \sigma^2(r_{23})\right)^{1/2} = 1.4125 \cdot 10^{-4} N.$$

So,

$$\vec{F}_{23} \pm \sigma(F_{23}) = +\widehat{x}(47.98 \pm 1.41) \cdot 10^{-4} N. \tag{21}$$

6.3

For the force F_{41} of the part with the number 1 (that is part DR of length $l_1 \pm \sigma l_1 = [(0.30 + 0.10) = 0.40 \pm 0.001]$ m) on the part with number 4 (that is part CD (of length 0.01 cm)), as is seen in figs. 1 and 2, we analyse each one of the two vectors $\vec{r}_{41}$ and $\mathrm{d}\vec{l_4}$ into two components along the perpendicular directions $\widehat{x}$ and $\widehat{y}$. $\widehat{y}$ is the unit vector along the direction y, which is normal to the direction of motion of the copper submarine (see figs. 1 and 2). That is,

$$\begin{aligned} \vec{r}_{41} &= r_{41,x}(-\widehat{x}) + r_{41,y}\widehat{y}, \\ \mathrm{d}\vec{l_4} &= \mathrm{d}l_{4,x}(-\widehat{x}) + \mathrm{d}l_{4,y}\widehat{y}, \end{aligned} \tag{22}$$

where $r_{41,x} \pm \sigma(r_{41,x}) = [(0.40 + 0.005) = 0.405 \pm 0.001]$ m, $r_{41,y} \pm \sigma r_{41,y} = (0.0015 \pm 0.00050)$ m and $l_{4,x} \pm \sigma l_{4,x} = (0.010 \pm 0.001)$ m, $l_{4,y} \pm \sigma l_{4,y} = (0.0015 \pm 0.00050)$ m. We also have $r_1 = (0.40/2)$ m $= 0.20$ m, $r_4 = (0.40 + 0.005)$ m $= 0.405$ m, and $r_{41} = r_4 - r_1 = (0.405 - 0.20)$ m $= 0.205$ m.

Using eq. (1) we have

$$\begin{aligned} \mathrm{d}^2\vec{F}_{41} &= -\frac{\mu_0}{4\pi} I_1 I_4 \frac{\vec{r}_{41}}{{r_{41}}^3}\left[2\mathrm{d}l_1 \cdot \mathrm{d}\vec{l_4} - \frac{3}{{r_{41}}^2}(\mathrm{d}\vec{l_1} \cdot \vec{r}_{41})(\mathrm{d}\vec{l_4} \cdot \vec{r}_{41})\right] \\ &= -\frac{\mu_0}{4\pi} I_1 I_4 \frac{[r_{41,x}(-\widehat{x}) + r_{41,y}\widehat{y}]}{({r_{41,x}}^2 + {r_{41,y}}^2)^{3/2}}\left\{\left[2\mathrm{d}l_1(-\widehat{x})\right] \cdot [\mathrm{d}l_{4,x}(-\widehat{x}) + \mathrm{d}l_{4,y}\widehat{y}]\right. \\ &\quad \left. - \frac{3\mathrm{d}l_1(-\widehat{x}) \cdot [r_{41,x}(-\widehat{x}) + r_{41,y}\widehat{y}][\mathrm{d}l_{4,x}(-\widehat{x}) + \mathrm{d}l_{4,y}\widehat{y}] \cdot [r_{41,x}(-\widehat{x}) + r_{41,y}\widehat{y}]}{{r_{41,x}}^2 + {r_{41,y}}^2}\right\} \\ &= -\frac{\mu_0}{4\pi} I_1 I_4 \left[\frac{r_{41,x}(-\widehat{x}) \cdot 2 \cdot \mathrm{d}l_1 \mathrm{d}l_{4,x} + r_{41,y}\widehat{y} \cdot 2 \cdot \mathrm{d}l_1 \mathrm{d}l_{4,x}}{({r_{41,x}}^2 + {r_{41,y}}^2)^{3/2}}\right. \\ &\quad - 3\frac{r_{41,x}(-\widehat{x})\mathrm{d}l_1 r_{41,x}\mathrm{d}l_{4,x}r_{41,x} + r_{41,x}(-\widehat{x})\mathrm{d}l_1 r_{41,x}\mathrm{d}l_{4,y}r_{41,y}}{({r_{41,x}}^2 + {r_{41,y}}^2)^{5/2}} \\ &\quad \left. -3\frac{r_{41,y}\widehat{y}\,\mathrm{d}l_1 r_{41,x}\mathrm{d}l_{4,x}r_{41,x} + r_{41,y}\widehat{y}\,\mathrm{d}l_1 r_{41,x}\mathrm{d}l_{4,y}r_{41,y}}{({r_{41,x}}^2 + {r_{41,y}}^2)^{5/2}}\right] \\ \Rightarrow \vec{F}_{41} &= -\frac{\mu_0}{4\pi} I_1 I_4 \left[\frac{r_{41,x}(-\widehat{x}) \cdot 2 \cdot \int_{-0.20}^{0.20}\mathrm{d}l_1 \int_{-0.005}^{0.005}\mathrm{d}l_{4,x} + r_{41,y}\widehat{y} \cdot 2 \cdot \int_{-0.20}^{0.20}\mathrm{d}l_1 \int_{-0.005}^{0.005}\mathrm{d}l_{4,x}}{({r_{41,x}}^2 + {r_{41,y}}^2)^{3/2}}\right. \\ &\quad - 3\frac{r_{41,x}(-\widehat{x})\int_{-0.20}^{0.20}\mathrm{d}l_1 \int_{-0.005}^{0.005}\mathrm{d}l_{4,x}r_{41,x}^2 + {r_{41,x}}^2(-\widehat{x})\int_{-0.20}^{0.20}\mathrm{d}l_1 \int_0^{0.0015}\mathrm{d}l_{4,y}r_{41,y}}{({r_{41,x}}^2 + {r_{41,y}}^2)^{5/2}} \\ &\quad \left. - 3\frac{r_{41,y}\widehat{y}\int_{-0.20}^{0.20}\mathrm{d}l_1 \int_{-0.005}^{0.005}\mathrm{d}l_{4,x}{r_{41,x}}^2 + r_{41,y}\widehat{y}\int_{-0.20}^{0.20}\mathrm{d}l_1 r_{41,x}\int_0^{0.0015}\mathrm{d}l_{4,y}r_{41,y}}{({r_{41,x}}^2 + {r_{41,y}}^2)^{5/2}}\right] \\ \Rightarrow F_{41,x} &= -10^{-7} \cdot 400 \cdot 400\left[\frac{-0.205 \cdot 2 \cdot 0.40 \cdot 0.01}{(0.205^2 + 0.0015^2)^{3/2}}\right. \\ &\quad \left. - 3\frac{-0.205^3 \cdot 0.40 \cdot 0.01 - 0.205^2 \cdot 0.40 \cdot 0.0015 \cdot 0.0015}{(0.205^2 + 0.0015^2)^{5/2}}\right] = -0.0015N. \end{aligned} \tag{23}$$

We have

$$\sigma(F_{41}) = \left(\left(\frac{\partial F_{41}}{\partial I_1}\right)^2 \sigma^2(I_1) + \left(\frac{\partial F_{41}}{\partial I_4}\right)^2 \sigma^2(I_4)\right)^{1/2} = 4.3206 \cdot 10^{-5}N.$$

So,

$$\vec{F}_{41,x} \pm \sigma(F_{41}) = -\widehat{x}(15.000 \pm 0.432) \cdot 10^{-4}N. \tag{24}$$

6.4

For the force F_{43} of the part with the number 3 (that is part CL of length $l_3 \pm \sigma l_3 = [(0.30\,\mathrm{m} + 0.15\,\mathrm{m} + 0.04\,\mathrm{m}) = 0.490\,\mathrm{m} \pm 0.001\,\mathrm{m}]$) on the part with the number 4 (that is, part CD of length 0.01 m), as is seen in fig. 1, we also

analyse each one of the two vectors $\vec{r}_{43}$ and $\mathrm{d}\vec{l_4}$ into two components along the perpendicular directions $\widehat{x}$ and $\widehat{y}$. $\widehat{y}$ is the unit vector along the direction y, which is normal to the direction of motion of the copper submarine (see fig. 1). That is,

$$\begin{aligned}\vec{r}_{43} &= r_{43,x}\widehat{x} + r_{43,y}\widehat{y},\\ \mathrm{d}\vec{l_4} &= \mathrm{d}l_{4,x}(-\widehat{x}) + \mathrm{d}l_{4,y}\widehat{y},\end{aligned} \tag{25}$$

where $r_{43,x} \pm \sigma(r_{43,x}) = (0.250 \pm 0.001)\,\mathrm{m}$, $r_{43,y} \pm \sigma r_{43,y} = (0.00150 \pm 0.00050)\,\mathrm{m}$ and $l_{4,x} \pm \sigma l_{4,x} = (0.010 \pm 0.001)\,\mathrm{m}$, $l_{4,y} \pm \sigma l_{4,y} = (0.00150 \pm 0.00050)\,\mathrm{m}$.

We have $r_3 = (0.300 + 0.100 + 0.010 + 0.245)\,\mathrm{m} = 0.655\,\mathrm{m}$, $r_4 = (0.300 + 0.100 + 0.010/2)\,\mathrm{m} = 0.405\,\mathrm{m}$ and $r_{43,x} = r_4 - r_3 = (0.405 - 0.655)\,\mathrm{m} = 0.250\,\mathrm{m}$.

Using eq. (1) we find

$$\begin{aligned}\mathrm{d}^2\vec{F}_{43} &= -\frac{\mu_0}{4\pi}I_4I_3\frac{(-\vec{r}_{43})}{{r_{43}}^3}\left[2\mathrm{d}l_3\cdot\mathrm{d}\vec{l_4} - \frac{3}{{r_{43}}^2}(\mathrm{d}\vec{l_3}\cdot\vec{r}_{43})(\mathrm{d}\vec{l_4}\cdot\vec{r}_{43})\right]\\
&= -\frac{\mu_0}{4\pi}I_4I_3\frac{(+r_{43,x}\widehat{x} + r_{43,y}\widehat{y})}{({r_{43,x}}^2 + {r_{43,y}}^2)^{3/2}}[2\mathrm{d}l_3(-\widehat{x})\cdot[\mathrm{d}l_{4,x}(-\widehat{x}) + \mathrm{d}l_{4,y}\widehat{y}]\\
&\quad - \frac{3\mathrm{d}l_3(-\widehat{x})\cdot(+r_{43,x}\widehat{x} + r_{43,y}\widehat{y})[\mathrm{d}l_{4,x}(-\widehat{x}) + \mathrm{d}l_{4,y}\widehat{y}]\cdot(+r_{43,x}\widehat{x} + r_{43,y}\widehat{y})}{{r_{43,x}}^2 + {r_{43,y}}^2}\\
&= -\frac{\mu_0}{4\pi}I_4I_3\left[\frac{+r_{43,x}\widehat{x}\cdot 2\cdot(-\mathrm{d}l_3)(-\mathrm{d}l_{4,x}) + r_{43,y}\widehat{y}\cdot 2\cdot\mathrm{d}l_3\mathrm{d}l_{4,x}}{({r_{41,x}}^2 + {r_{41,y}}^2)^{3/2}}\right.\\
&\quad - 3\frac{+r_{43,x}\widehat{x}\,\mathrm{d}l_3 r_{43,x}\mathrm{d}l_{4,x}r_{43,x} - r_{43,x}\widehat{x}\,\mathrm{d}l_3 r_{43,x}\mathrm{d}l_{4,y}r_{43,y}}{({r_{43,x}}^2 + {r_{43,y}}^2)^{5/2}}\\
&\quad \left. - 3\,\frac{-r_{43,y}\widehat{y}\,\mathrm{d}l_3 r_{43,x}\mathrm{d}l_{4,x}r_{43,x} - r_{43,y}\widehat{y}\,\mathrm{d}l_3 r_{43,x}\mathrm{d}l_{4,y}r_{43,y}}{({r_{43,x}}^2 + {r_{43,y}}^2)^{5/2}}\right]\\
\Rightarrow F_{43} &= -\frac{\mu_0}{4\pi}I_4I_3\left[\frac{+r_{43,x}\widehat{x}\cdot 2\cdot\int_{-0.245}^{0.245}\mathrm{d}l_3\int_{-0.005}^{0.005}\mathrm{d}l_{4,x} - r_{43,y}\widehat{y}\cdot 2\cdot\int_{-0.245}^{0.245}\mathrm{d}l_3\int_{-0.005}^{0.005}\mathrm{d}l_{4,x}}{({r_{43,x}}^2 + {r_{43,y}}^2)^{3/2}}\right.\\
&\quad - 3\frac{+r_{43,x}\widehat{x}\int_{-0.245}^{0.245}\mathrm{d}l_3\int_{-0.005}^{0.005}\mathrm{d}l_{4,x}{r_{43,x}}^2 - {r_{43,x}}^2\widehat{x}\int_{-0.245}^{0.245}\mathrm{d}l_3\int_{0}^{0.0015}\mathrm{d}l_{4,y}r_{43,y}}{({r_{43,x}}^2 + {r_{43,y}}^2)^{5/2}}\\
&\quad \left. - 3\,\frac{-r_{43,y}\widehat{y}\int_{-0.245}^{0.245}\mathrm{d}l_3\int_{-0.005}^{0.005}\mathrm{d}l_{4,x}{r_{43,x}}^2 - r_{43,y}\widehat{y}\int_{-0.245}^{0.245}\mathrm{d}l_3 r_{43,x}\int_{0}^{0.0015}\mathrm{d}l_{4,y}r_{43,y}}{({r_{43,x}}^2 + {r_{43,y}}^2)^{5/2}}\right]\\
\Rightarrow F_{43,x} &= -10^{-7}400\cdot 400\left[\frac{+0.25\cdot 2\cdot 0.49\cdot 0.01}{(0.25^2 + 0.0015^2)^{3/2}}\right.\\
&\quad \left. - 3\,\frac{+0.25^3\cdot 0.49\cdot 0.01 - 0.25^2\cdot 0.49\cdot 0.0015\cdot 0.0015}{(0.25^2 + 0.0015^2)^{5/2}}\right] = +0.0013N.\end{aligned} \tag{26}$$

We have

$$\sigma(F_{43}) = \left(\left(\frac{\partial F_{43}}{\partial I_3}\right)^2\sigma^2(I_3) + \left(\frac{\partial F_{43}}{\partial I_4}\right)^2\sigma^2(I_4)\right)^{1/2} = 3.5378\cdot 10^{-5}N.$$

So,

$$\vec{F}_{43,x} \pm \sigma(F_{43,x}) = +\widehat{x}(13.000 \pm 0.354)\cdot 10^{-4}N. \tag{27}$$

We have found that the forces $\vec{F}_{21}$ and $F_{41,x}\cdot\widehat{x}$ are in the direction of the $-\widehat{x}$-axis, which is in the direction of the motion of the copper submarine, while the forces $\vec{F}_{23}$ and $F_{43,x}\cdot\widehat{x}$ are in the direction of the $+\widehat{x}$-axis. We also see that the sum of the absolute values of the forces $\vec{F}_{21}$ and $F_{41,x}\cdot\widehat{x}$ is bigger than the sum of the absolute values of the forces $\vec{F}_{23}$ and $F_{43,x}\cdot\widehat{x}$. So the resultant of the forces $\vec{F}_{21}$ and $F_{41,x}\cdot\widehat{x}$ and $\vec{F}_{23}$ and $F_{43,x}\cdot\widehat{x}$ is in the direction of the motion of the projectile ($-\widehat{x}$-axis).

For the total Ampère force acting on the copper submarine we obtain

$$\begin{aligned}\vec{F}_{\text{total-Ampère}} &= \vec{F}_{21} + F_{41,x}\cdot\widehat{x} + \vec{F}_{23} + F_{43,x}\cdot\widehat{x}\\ &= [-\widehat{x}\cdot 0.005183 - \widehat{x}\cdot 0.0015 + \widehat{x}\cdot 0.004798 + \widehat{x}\cdot 0.0013]N\\ &= (-3.85\cdot 10^{-4}\cdot\widehat{x} - 2.77\cdot 10^{-4}\cdot\widehat{x})N = -6.62\cdot 10^{-4}\cdot\widehat{x}N.\end{aligned}$$

We find

$$\sigma F_{\text{total-Ampère}} = \sqrt{\sigma^2 F_{21} + \sigma^2 F_{41} + \sigma^2 F_{23} + \sigma^2 F_{43}} = 2.16\cdot 10^{-4}N.$$

So,

$$\vec{F}_{\text{total-Ampère}} \pm \sigma(F_{\text{total-Ampère}}) = -\widehat{x}(6.62\cdot 10^{-4} \pm 2.16\cdot 10^{-4})N. \tag{28}$$

7 Calculation of the velocity according to the Ampère force law

We have

$$F_{\text{total-Ampère}} = 6.62\cdot 10^{-4}N = 0.5\cdot\rho\cdot C_A\cdot A_0\cdot \upsilon_x^2 \tag{29}$$

Solving for υ_x we find

$$\upsilon_x = \sqrt{\frac{F_{\text{total-Ampère}}}{0.5\rho C_A A_0}} = \sqrt{\frac{6.62\cdot 10^{-4}N}{0.5\cdot 13545.7(\,\text{kg/m}^3)(0.90)\pi(1.5\cdot 10^{-3})^2\,\text{m}^2}} = 0.124(\,\text{m/s}).$$

We have $\sigma(\upsilon_x^2) = \sqrt{\left(\frac{\partial {\upsilon_x}^2}{\partial F_{\text{total}}}\right)^2\sigma^2(F_{\text{total}}) + \left(\frac{\partial {\upsilon_x}^2}{\partial C_A}\right)^2\sigma^2(C_A)} = 0.0085\,\text{m}^2/\text{s}^2$ and $\sigma(\upsilon_x) = 0.092\,\text{m/s}$.

Thus we find, using the Ampère force law,

$$\upsilon_x \pm \sigma(\upsilon_x) = (0.12 \pm 0.09)\,\text{m/s}. \tag{30}$$

8 The longitudinal Ampère and B-S-G-L forces in the case both ends of the wire are squared off

It has been proved theoretically and experimentally that "In a closed circuit the force acted on a part of the circuit by the rest of the circuit it turns out to be identical whether calculated by using the Biot-Savart-Faraday-Lorentz force law or by using the Ampère force law", since the Ampère and Biot-Savart-Faraday-Lorentz force laws are in this aspect equivalent [33,42,44,45].

The form of Ampère's force law using volume elements and current densities is eq. (1). The sixfold integral law reduces to the following twofold integral in the case the current elements $\mathrm{d}\vec{l}_1$ and $\mathrm{d}\vec{l}_2$ lie on the same straight line, are parallel between them, are in the same direction, and have the same cross-section (see fig. 5),

$$\mathrm{d}^2\vec{F}_{21} = k\vec{r}_{21}\mathrm{d}l_1\mathrm{d}l_2/{r_{21}}^3$$

or

$$\mathrm{d}^2F_{21} = k\mathrm{d}l_1\mathrm{d}l_2/{r_{21}}^2\,, \tag{31}$$

where

$$k = [\mu_0/(4\pi)]I_1I_2,$$

taking into account that the dot products $\mathrm{d}\vec{l}_1\cdot\mathrm{d}\vec{l}_2$ and $(\mathrm{d}\vec{l}_1\cdot\vec{r}_{21})(\mathrm{d}\vec{l}_2\cdot\vec{r}_{21})$ become $(\mathrm{d}l_1)(\mathrm{d}l_2)$ and $(\mathrm{d}l_1 r_{21})(\mathrm{d}l_2 r_{21})$. The vector distance, $\vec{r}_{21}$, between the centres of the current elements $\mathrm{d}\vec{l}_1$ and $\mathrm{d}\vec{l}_2$, lies on the same straight line as $\mathrm{d}\vec{l}_1$ and $\mathrm{d}\vec{l}_2$ and is parallel to them (see fig. 5).

Integrating eq. (31) we obtain

$$F_{21} = kl_1l_2/{r_{21}}^2. \tag{32}$$

This is the longitudinal Ampère force of $\vec{l}_1$ on $\vec{l}_2$.

Taking into account the B-S-G-L force law, eq. (2), we see that the vector product, $\mathrm{d}\vec{l}_1\times\vec{r}_{21} = 0$, since $\mathrm{d}\vec{l}_1$ and $\vec{r}_{21}$ are parallel (see fig. 5). Thus, it seems that the B-S-G-L force law does not predict any longitudinal forces.

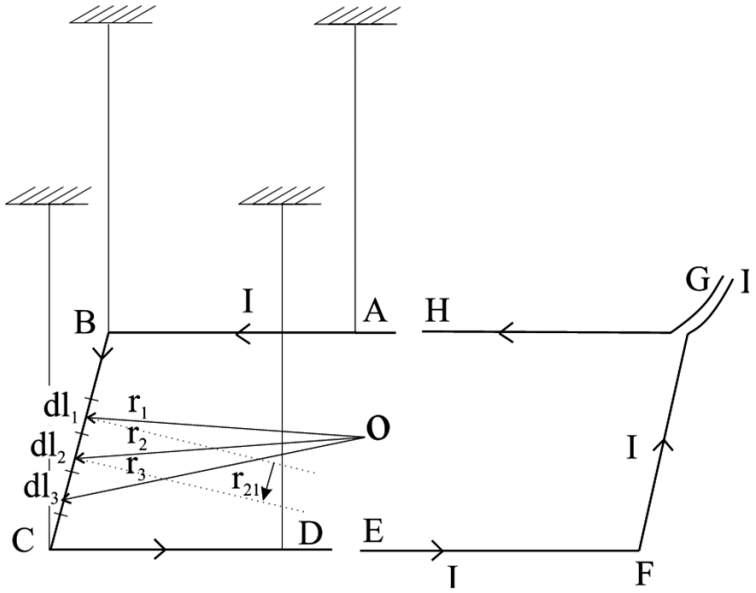

Fig. 5. The principle of the pendulum experiments. EFGH is the stationary part while ABCD is the moving part. The current elements $\mathrm{d}l_1$ and $\mathrm{d}l_2$, along with their distance r_{21}, from the coordinate's origin O are seen.

9 Conclusions

9.1

Taking into account eqs. (11) and (28) we see that i) both force laws, that of B-S-G-L and that of Ampère, anticipate, within the calculated error, the same force acting on the projectile submarine. Based on this result we have also shown that ii) the theoretically calculated velocity of the submarine, υ_x, by using the B-S-G-L and Ampère force laws, is in complete agreement, within the calculated error, with the velocity υ_x experimentally measured by the experimenters of the submarine (see eqs. (17) and (30)).

9.2

In [4] P. Graneau states: "... Strong evidence of tensile breaks, prior to melting and evaporation of the wire, were found in an experiment [5]. None of [5] photographs show the neck formation which is a feature of static tensile strength tests. When the evidence of the experiments of mine is combined with Nasilowski's findings [5], there remain little doubt that the observed wire fragmentation was the result of tensile fracture in the solid state of copper and aluminum wires ..." Also, in [29], P. Graneau *et al.* stated: "... Without knowledge of longitudinal Ampère forces, investigators had no choice but to attribute filament rupture to an $m = 0$ MHD instability. This phenomenon forms a neck in the filament, and the consequent radial current components on both sides of the neck repel each other and fracture the plasma column ..."

The author of the present work believes that the neck formation before the wire fragmentation is the ideal case for the subsequent creation of longitudinal B-S-G-L forces (see introduction).

9.3

As we have seen in the experiment of ref. [1] P. Graneau found that the projectile is moving along the direction of the current, longitudinally, when it is placed on the surface of a straight mercury trough and a current of $I = 400\,\mathrm{A}$ flows along the mercury trough. Therefore, it is inconceivable to state that there are no longitudinal forces. See ref. [38].

In sect. 3 of the present work we have revealed the mechanism for the creation of longitudinal forces by the B-S-G-L force law and, in sect. 6, we have presented the calculations for the longitudinal forces according to the Ampère force law. We have seen that both force laws, that of B-S-G-L and that of Ampère, anticipate, within the calculated error, the same force acting on the projectile submarine. This is not accidental since, in sect. 5, where we present the theoretical calculation of the velocity $\upsilon_x[= 0.15\,\mathrm{m/s}]$, along the $-x$-axis, according to the Biot-Savart-Grassmann-Lorentz force law, and, in sect. 7, where we present the calculation for the velocity according to the Ampère force law, we have found

that this velocity is in complete agreement, within the calculated error, with the velocity experimentally measured by the experimenters ($v_x = 0.15\,\mathrm{m/s}$).

9.4

Relativity theory, considering the transformation laws for E and B, for the magnetic field produced by a moving charge q, gives

$$B = \frac{q \cdot \gamma \cdot v \times r}{c\,(y^2 + \gamma^2 \cdot x^2)^{3/2}},$$
$$\gamma = \left(1 - v^2/c^2\right)^{-1/2}.$$

This formula has the following consequences:
a) For $v \ll c$, which actually is our case of metallic conductors, the above formula implies

$$\mathbf{B} = \frac{q \cdot v \times r}{c \cdot r^2}.$$

This is just the Biot-Savart law, for Ids $\sim qv$. It follows, therefore, that the relativity theory approximates, adequately enough in our case of metallic conductors, the Biot-Savart law.
b) In general, relativity theory does not imply the Biot-Savart law independently of the velocity of individual charges.

9.5

The average speed of electrons in a wire in which a high current density is flowing, the so-called drift velocity, is of the order of $0.01\,\mathrm{m/s}$. We can obtain the Biot-Savart-Grassmann (B-S-G) force law by a combination of Laplace's second law,

$$\mathrm{d}^2 F_2 = I_2 \cdot \mathrm{d}s_2 \times \mathrm{d}B,$$

with Laplace's first law,

$$\mathrm{d}B = \frac{\mu_0}{4\pi} I_1 \cdot \mathrm{d}s_1 \times \frac{\vec{r}}{r^2},$$

thus deriving the B-S-G force law,

$$\mathrm{d}^2 F_2 = \frac{\mu_0}{4\pi\rho^2} I_1 I_2 \mathrm{d}s_2 \times (\mathrm{d}s_1 \times \vec{r}).$$

The Lorentz force law, $\mathrm{d}F = \mathrm{d}q \cdot v \times B$, is equivalent to Laplace's second law. We point out that Laplace's first law is an approximation to the Lienard-Wiechert law for $v/c \to 0$ and for negligible acceleration $\mathbf{a}$. The Lienard-Wiechert law is the solution to the Maxwell equations for a pointlike electric charge q.

There are very accurate experiments on accelerated electrons as those in modern synchrotrons. These experiments show that the Lorentz force (equivalent to Laplace's second law) is always valid but the field produced by accelerated charges is given by the complete solutions of Lienard and Wiechert. Consequently, Laplace's first law, and thus the B-S-G force law, is no longer valid in these cases since it is an approximation of the Lienard-Wiechert solution not only for $v \ll c$ but also because it neglects the acceleration (or radiation) term. It is the latter term that produces the radiation of electromagnetic waves and, in the case of synchrotrons, the recently well-studied synchrotron light [33, 37,38]. Ampère's electrodynamics gives no hints as to how to face radiation. It is an *ad hoc* formula.

9.6

Today, as far as the Newton's Theory is concerned the General Theory of Relativity prevails, which expresses gravity on the basis of the Special Theory of Relativity (finite maximum velocity). On this basis Classical Electrodynamics, which has been formulated by Maxwell, has ceased to present conceptual problems and it is understood as Field Theory. Now we believe that Classical Electrodynamics cannot be interpreted so as to incorporate action at a distance (as the Ampère force law); it is a Field Theory.

9.7

As we have mentioned earlier it was known to the scientific community that Ampère's and the Biot-Savart-Grassmann-Lorentz force laws were equivalent in all other aspects except for the fact that the Ampère force law predicted longitudinal forces between two current elements while B-S-G-L force law did not.

Based on the above two effects (that is, a) the fact that both force laws anticipate the same force acting on the projectile and b) the fact that the theoretically calculated velocity of the submarine, v_x, by using both force laws, is in complete agreement with the velocity of the submarine experimentally measured by the experimenters) the present work explains the mechanism for the creation of longitudinal forces by the B-S-G-L force law. Thus, it shows the complete equivalence of the latter law, in all aspects, with the Ampère force law.

References

1. P. Graneau, Nature **295**, 311 (1982).
2. P. Graneau, J. Appl. Phys. **53**, 6648 (1982).
3. P.T. Pappas, Nuovo Cimento B **76**, 189 (1983).
4. P. Graneau, Phys. Lett. A **97**, 253 (1983).
5. J. Nasilowski, in *Exploding wires*, edited by W.G. Chace, H.K. Moore, Vol. **3** (Plenum, New York, 1964) p. 295.
6. P. Graneau, J. Appl. Phys. **55**, 2598 (1984).
7. P. Graneau, IEEE Trans. Magn. **20**, 444 (1984).
8. K.H. Carpenter, IEEE Trans. Magn. **20**, 2159 (1984).
9. H. Aspden, Phys. Lett. A **107**, 238 (1985).
10. J.G. Ternan, J. Appl. Phys. **57**, 1743 (1985).
11. P. Graneau, P.N. Graneau, Appl. Phys. Lett. **46**, 468 (1985).
12. P. Graneau, J. Appl. Phys. **58**, 3638 (1985).
13. J.G. Ternan, J. Appl. Phys. **58**, 3639 (1985).
14. J.G. Ternan, Phys. Lett. A **115**, 230 (1986).
15. R. Azevedo *et al.*, Phys. Lett. A **117**, 101 (1986).
16. P. Graneau, Phys. Lett. A **120**, 77 (1987).
17. L. Dragone, J. Appl. Phys. **62**, 3477 (1987).
18. P. Graneau, J. Appl. Phys. **62**, 3006 (1987).
19. V. Peoglos, J. Phys. D: Appl. Phys. **21**, 1055 (1988).
20. C. Christodoulides, Am. J. Phys. **56**, 357 (1988).
21. J. Nasilowski, IEEE Trans. Magn. **24**, 3260 (1988).
22. P. Graneau, J. Phys. D: Appl. Phys. **22**, 1083 (1988).
23. P. Graneau, IEEE Trans. Magn. **25**, 3275 (1989).
24. T.E. Phipps, T.E. Phipps, Jr., Phys. Lett. A **146**, 6 (1990).
25. M. Rambaut, J.P. Vigier, Phys. Lett. A **148**, 229 (1990).
26. M. Rambaut, Phys. Lett. A **154**, 210 (1991).
27. M. Rambaut, Phys. Lett. A **163**, 335 (1992).
28. M. Rambaut, Phys. Lett. A **164**, 155 (1992).
29. P. Graneau, N. Graneau, Phys. Lett. A **165**, 1 (1992).
30. P. Graneau, N. Graneau, Phys. Lett. A **174**, 421 (1993).
31. N. Graneau, IEEE Trans. Plasma Sci. **21**, 701 (1993).
32. P. Graneau, N. Graneau, IEEE Trans. Magn. **33**, 4570 (1997).
33. G. Cavalleri, G. Bettoni, E. Tonni, G. Spavieri, Phys. Rev. E **58**, 2505 (1998).
34. G. Cavalleri, E. Tonni, Phys. Rev. E **62**, 7545 (2000).
35. N. Graneau, T. Phipps, D. Roscoe, Eur. Phys. J. D **15**, 87 (2001).
36. P. Graneau, N. Graneau, Phys. Rev. E **63**, 058601 (2001).
37. G. Cavalleri, E. Tonni, G. Spavieri, Phys. Rev. E **63**, 058602 (2001).
38. G. Cavalleri, E. Cesaroni, E. Tonni, G. Spavieri, Eur. Phys. J. D **26**, 221 (2003).
39. G. Ajoy, Phys. Rev. E **74**, 067602 (2006).
40. G. Cavalleri, E. Cesaroni, E. Tonni, G. Spavieri, Eur. Phys. J. D **42**, 407 (2007).
41. A.M. Ampère, *Memoires de l'Academie Royale des Sciences* (1827) (Ampère's equation was submitted to the French Academy of Sciences in 1823) and A.M. Ampère, *Memoires sur l'Electrodynamique*, Vol. **1** (Gauthier-Villars, Paris, 1882) p. 25.
42. P.G. Moyssides, IEEE Trans. Magn. **25**, 4307 (1989).
43. James Clerk Maxwell, *Treatise on Electricity and Magnetism* (Oxford, 1891) and Vol. 2 (New York, 1954) article 528, p. 175.
44. P.G. Moyssides, IEEE Trans. Magn. **25**, 4298 (1989).
45. P.G. Moyssides, IEEE Trans. Magn. **25**, 4313 (1989) and G. Diamantakos, G. Stratakis, PhD thesis (National Technical University of Athens, 1987).